2023 8th International Conference on Robotics and Automation Engineering

An Automated Framework for Drone-based Solar Panel Soiling Detection

Zac Brydon
School of Information Technology
Deakin University
Melbourne, Australia
zbrydon@deakin.edu.au

Kevin Lee
School of Information Technology
Deakin University
Melbourne, Australia
kevin.lee@deakin.edu.au

Alireza Hassani
Car Advance Ivanhoe,
Australia
ah@caradvance.com.au

2023 8th International Conference on Robotics and Automation Engineering (ICRAE) | 979-8-3503-2765-6/23/$31.00 ©2023 IEEE | DOI: 10.1109/ICRAE59816.2023.10458606

***Abstract*—The installation of both residential and commercial photovoltaic cells (PVs) has been growing rapidly. In either situation maximising the efficiency of the PVs is critical this can be hindered by soiling, cracks, and other defects. Detecting such faults through regular inspections is an essential yet costly task for small and large scale PVs deployments. The research presented in this paper proposes a drone-based system that navigates a PVs installation, capturing an image and the location of the panels. Machine Learning is then used to detect any instances of soiling or visual faults, these locations can then be used by a cleaning robot or a maintenance team depending on the type of damage or soiling. The proposed approach is evaluated using real deployed PV cell arrays, demonstrating it as an effective solution for detecting PV soiling.**

***Index Terms*—Solar Panel, Computer Vision, Framework, Soiling Detection, Drone, Automated**

I. Introduction

As the worlds energy requirements grow [1], it is increasingly important to find an energy production method that is sustainable and renewable. Photovoltaic cells in the form of solar panels are one of the most extensively used forms of renewable energy and there is a strong future for the technology [2], with the increase of installations across the globe in the last decade. This trend is likely to continue with the global primary energy demands predicted to be made up of 27% solar energy by 2070 [3].

Solar panel energy output can be hindered by environmental factors, one of which being the accumulation of dust on the panels surface. This is a significant issue considering the expected contributions to the energy demands of the globe that solar will make, and that many of the locations most viable for Photovoltaic deployments are subject to large or frequent amounts of dust [4]. This can result in efficiency drops of up to 22% [5], [6] since panels are commonly wired in series meaning it only takes one panel to be affected for the whole modules efficiency to be affected. Solar panels can also be subject to faults, whether due to harsh operating environments or errors in their production. These faults can include cracks, delamination, snail trails and discolorations. Depending on the type and extent of the fault can either reduce the panels power output or render the panel defective.

To ensure that current and future deployments of Solar panels are kept operating at peak efficiency, the panels surface has to be inspected and cleaned. Many methods for solar panel detection and inspection exist, including manual inspection, laser detection, infrared thermography. The manual inspection of solar panels in a large power station isn't viable due to the shear quantity of panels. Laser detection methods focus on the detection of faults in panels at manufacturing time which is not a suitable solution for panels that have already been in operation for many years. A promising area of research is fault detection using vision, both infrared and visible light, that can be applied universally to any PV panel installations.

The aim of the research presented in this paper is to investigate techniques and propose an optimal architecture for detecting solar panels and their physical status using drones. This approach will allow the design and development of a complete drone-based system that detects soiled or faulty PV modules in varying sizes of PV installations. The contributions of this paper are: (i) digital image processing methods for the detection of arrays of solar panel arrays, panels and cells, (ii) an automated framework for drone-based PV soiling detection.

Section II presents a review of the literature. Section III describes TRANSECT, an automatic solar panel soiling detection framework. Section IV presents an evaluation of the system. Section IV-C presents a discussion on the real world suitability of this drone-based framework. Finally, Section V presents some conclusions and future work.

II. Background

The output of PV cells is highly dependent on the state of the panels, including the prescience of damage or dust. Efficient systems will have to be developed to ensure that both the existing and also future PV installations are regularly monitored so the necessary maintenance can be performed. Currently, this is a manual process involving with technicians visually inspecting PVs. One possible approach is to take imagery of PV arrays and analyse this to determine their current state. Computer Vision is the process by which computers attain a broad understanding of digital images, essentially attempting to automate the functionality of the human eye. In this particular application the objective is to detect solar panels in images, extract the panels and determine if there

is any difference between the characteristics of the detected solar panel and those of a panel known to be functioning correctly. To achieve this, the most common method used is edge detection because it is relatively simple due to the reduced data processing requirements, while simultaneously retaining the structural data of the objects edges [7].

To determine which object within the digital image is the desired target of the edge detection a threshold is usually applied, extracting the areas of the image with the expected color of the target object. Various color spaces exist for the segmentation of images including RGB (Red, Green, Blue), HSL (Hue, Saturation, Lightness) and HSV (Hue, Saturation, Value). RGB isn't the best for this application due to its chrominance and luminance values are combined, making it difficult to identify the same color under different lighting environments [8]. The HSV color space however separates these values, where hue is the main color value, saturation being how bright the color is and value representing the luminance. Reducing the noise of the resultant binary image is done with a Gaussian Filter [9], to identify the objects edges a border following algorithm is deployed [10].

Multiple image processing methods can be used for detecting soiling of PV modules, including segmentation, thresholding, edge segmentation, and region segmentation [11]. Region segmentation was found to produce better results when identifying instances of uniform soiling, whereas edge segmentation was most effective for PV modules experiencing nonuniform soiling. Yap [12] concluded that Lee's [13] algorithm which block matches was the most accurate in both the control and photograph image tests. In these experiments were conducted using a single yellow dust to soil the panels, in reality soiling can take many forms, such as droppings from flora and fauna. In order for these image processing techniques to be applied to images of many different PV modules, approaches need to consider the variety of soiling.

Convolutional Neural Networks (CNN) have been demonstrated to detect both soiling and faults. DeepSolarEye [14] uses RGB images and environmental factions (solar irradiance and time), to estimate the power lose experienced by the PV module, the soiling type and localisation. This system solves the detection portion of the problem of detecting and locating soiled or faulty PV panels in a large PV installation. Shihavuddin [15] compared CNN performance in detecting soiling and faults of both wind turbines and PV panels. This study used four different image sets, three of solar panels, one of which being a subset of Mehta et al. [14] images, and one of wind turbines. When detecting faults and soiling exclusively on PV panels the EfficientDet - D5 [16] deep learning object detection framework performed the best.

Cavieres et al. [17] uses RGB images and environmental data to predict the energy loss of a PV module. It does this by identifying and pulling each defective PV module from within a RGB image. The panels operating condition is then analysed and compared to a 'healthy' PV module that is operating in the same conditions. Henry et al. [18] proposes an automatic detection system uses an aerial drone to capture both RGB and IR images. The drones flight path is calculated by using a satellite image or an orthomosaic of the entire PV installation to detect the locations of the PV arrays. Once the drone has captured the images of the entire PV installation, the PV modules are analysed for defects using the maximum, minimum and average temperature of each of the modules.

III. TRANSECT: An Automatic Solar Panel Soiling Detection Framework

A. Overview

In this paper, we propose a system, named TRANSECT, that detects arrays of solar panels from digital images, the panels of each array are then detected and extracted, it then detects the cells within each panel, from which the detected number of cells can be compared to the expected number of cells to determine the state of the solar panels surface. The systems works using live video streamed from teleoperated or fully automated drones.

B. System Aims

The aim of the proposed system is to combine multiple digital image processing techniques to create detection pipelines for detecting arrays of solar panels, solar panels and the cells within them. These pipelines will be employed in a larger architecture to detect solar panels and their physical status, with the final objective being to design, develop and test a complete system that detects soiled or faulty PV modules in varying sizes of PV installations, with the following requirements.

- Req 1: The system must detect and extract arrays of solar panels from digital images.
- Req 2: The system must be able to distinguish between the panels in an array of panels.
- Req 3: The system must be able to estimate the amount of soiling present on an array of solar panels by analysing an image of it.
- Req 4: The system must be able to locate the panels that are affected by soiling.

C. Solar Panel Detection Approach

The proposed system architecture, illustrated in Figure 1, uses image processing techniques, including a HSV conversion, blue or black color range extraction, Gaussian filter, and binary threshold. In this, the original image is converted to the Hue, Saturation, Value color space (HSV), to separate the color component (Hue) and the intensity component (Value and Saturation) of the image. Changes in lighting conditions impact intensity rather than the color allowing for more accurate color segmentation of the image.

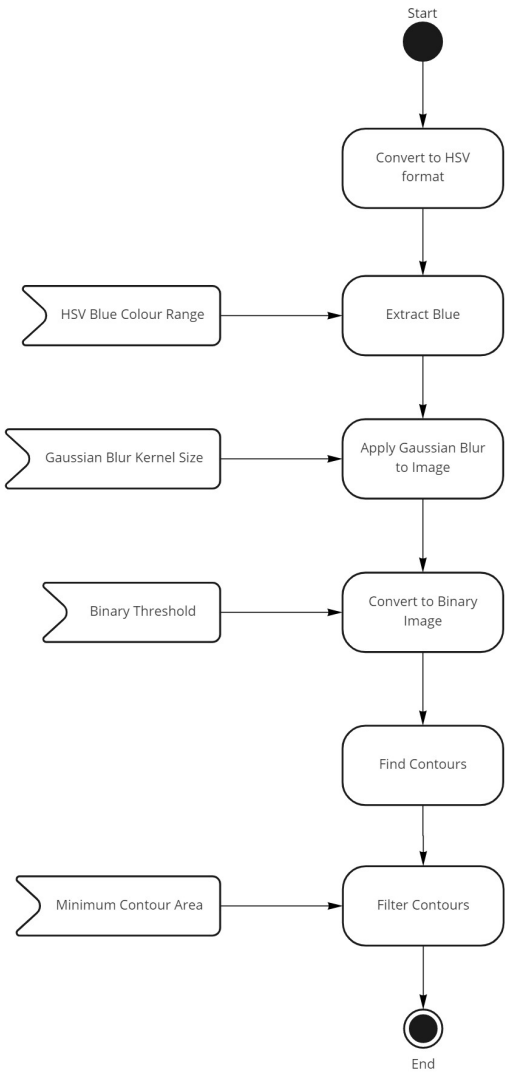

Fig. 1. Default Detection Setup

The blue or black is then extracted from the image, the HSV color ranges of blue and black are defined in Table III-C. OpenCV represents Hue, Value and Saturation with the ranges 0-179, 0-255 and 0-255 respectively. If a pixel has a HSV color value in the range Table III-C, then that pixel is set to 255, otherwise it is set to zero, creating a threshold image.

TABLE I
THE DEFAULT HSV COLOR RANGES.

	Hue	Saturation	Value
Blue Lower	75	0	0
Blue Upper	140	255	255
Black Lower	0	0	0
Black Upper	180	255	30

The image is smoothed to reduce the noise present in the image, this is done by applying a Gaussian filter to the threshold image. The default Gaussian Kernel size used is (7,7). It is then again converted to a binary image using a default threshold value of 60. This sets every pixel in the gray scale image with a value greater than the threshold to 255 otherwise the pixels value is set to zero.

Contours are created along the border of black and white pixels using the algorithm [10], which are then filtered by area. The default minimum contour area was set to 5000. The images used in the initial proof of concept testing of the system were selected from Google Image search for 'solar panels'.

D. Solar Panel Array Detection

For solar panel array detection, first, the the default process was used. Table II highlights that the HSV blue threshold lower boundary Value and Saturation was raised to gain a better distinction between the arrays, by further excluding the darker gaps between the arrays and the lighter borders of the arrays from the threshold. it also displays that the default color range of black was modified to detect the non-perfect black of the solar panels.

TABLE II
HSV COLOR RANGE FOR DETECTING ARRAYS OF PANELS.

	Hue	Saturation	Value
Blue Lower	70	60	80
Blue Upper	140	255	255
Black Lower	100	25	35
Black Upper	130	80	80

The minimum contour area was lowered to 2000 to allow for the detection of the arrays further away in the image. The Gaussian Blur Kernel size was reduced to (5,5), in order to avoid blurring the image leading to array merging.

E. Individual Solar Panel Detection

The default method was modified for detecting individual panels in an image. The Gaussian Blurring step was disabled unless the algorithm failed to detect more than the minimum expected panel count of five. The minimum detected contour area was then lowered from 1000 to 500, Gaussian Blurring with a kernel size of (7,7) was applied to the image and the contours were detected again. The HSV color threshold for blue and black was also modified for this application, as depicted in Table III, this was do to allow for greater distinction between the blue and black of the panels and the dark shadows and silver edges that border them.

TABLE III
HSV COLOR RANGE FOR DETECTING SOLAR PANELS.

	Hue	Saturation	Value
Blue Lower	70	70	60
Blue Upper	140	255	240
Black Lower	100	20	40
Black Upper	130	85	140

An additional method to detect the corners [19] of the detected panels was added to the default setup. These corner coordinates were then used to transform the possibly warped panels into rectangles for detecting the number of cells.

F. Solar Cell Detection

This system aims to take the transformed panels extracted from the panel detection system and apply a narrower HSV blue and black color range, shown in Table IV, to filter and then detect the individual cells present in the panel. It achieves this by using the same process as described in Section III-E to detect the cells and identify the corners of each cell, only differing in the HSV range.

TABLE IV
HSV COLOR RANGE FOR DETECTING CELLS WITHIN SOLAR PANELS.

	Hue	Saturation	Value
Blue Lower	100	100	100
Blue Upper	140	200	235
Black Lower	100	25	35
Black Upper	130	280	80

G. System Design

The base system architecture, shown in Figure 2 is consistent for both blue and black panels and the four different input types. First the selected input image is taken by the Array Detection, if any array is detected is is returned as an re-projected image, which is in turn used as input foe the panel detection module. Each panel is then used as individual input for the cell detection module, the final cell count is then calculated by counting the array of each panels cell contours. Each of the array, panel and cell detection modules are all variations on similar methods as seen in Section III-C.

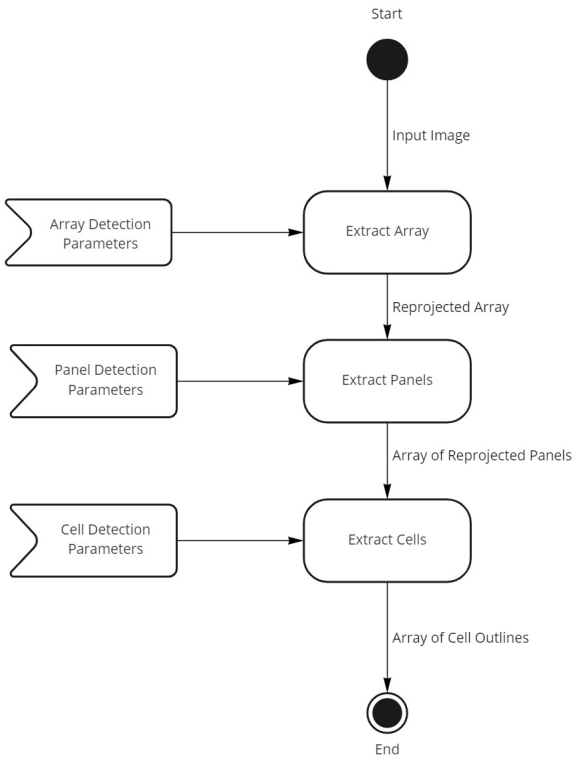

Fig. 2. High level architecture of TRANSECT

The Driver class gets the configuration data from user input or a JSON file. If the input type is defined as an image, a collection of images or a saved video the driver class instantiates ArrayDetection, PanelDetection and CellDetection objects. The input image or video frame is then passed to the ArrayDetection object which outputs the largest array in the image, this is extracted and re-projected, then used as input for the PanelDetection object. Each panel is then extracted and re-projected for the detection of each of the panels cells. Each object relies on the same base of image processing methods, just with parameters tailored to the specific detection type. The detection results are then printed to the command line, and written to a csv file for future analysis.

H. Algorithm

Blue or black is extracted from the image, the HSV color ranges of blue and black are defined in Tables II, III and IV. OpenCV represents Hue, Value and Saturation with the ranges 0-179, 0-255 and 0-255 respectively. If a pixel has a HSV value in the defined color ranges, then that pixel is set to 255, otherwise it is set to zero, creating a threshold image.

The image can then be smoothed to reduce the noise present in the image by applying a Gaussian filter to the threshold image. The default Gaussian Kernel size used is (7,7). After the image has been smoothed it is once again converted to a binary image using a default threshold value of 60. This sets every pixel in the grey scale image with a value greater than the threshold to 255 otherwise the pixels value is set to zero.

Contours are then created along the border of the black and white pixels using the algorithm [10], which are then filtered by area. The default minimum contour area is set to 5000. The corners of each detected contour are calculated by iterating over the pixels to find the sub-pixel accurate location of corners or radial saddle points, as described in the algorithm proposed by [20].

To re-project the detected array and panels the corners are passed to OpenCV's warpPerspective method, which applies a perspective transformation to the image using the formula:

$$dst(x, y) = src(\frac{M_{11}x+M_{12}y+M_{13}}{M_{31}x+M_{32}y+M_{33}}, \frac{M_{21}x+M_{22}y+M_{23}}{M_{31}x+M_{32}y+M_{33}})$$

I. System Deployment and Applications

The system supports two modes, either the user specifies the system configuration data manually via the CLI, as follows.

```
$ python3 Driver.py -gui
```

The system can also be run in headless mode, which relies on a JSON configuration input file, as follows.

```
$  python3 Driver.py -input input.json
```

If the input type is defined to be the live video stream from a DJI Tello drone, seen in Figure 4, a Drone object is created. Which establishes the connection to the drone via WiFi, and starts receiving the video stream. Each frame is then used as input and goes through the Array, Panel and cell detection process. If there is no array detected the system does not attempt to detect panels of cells.

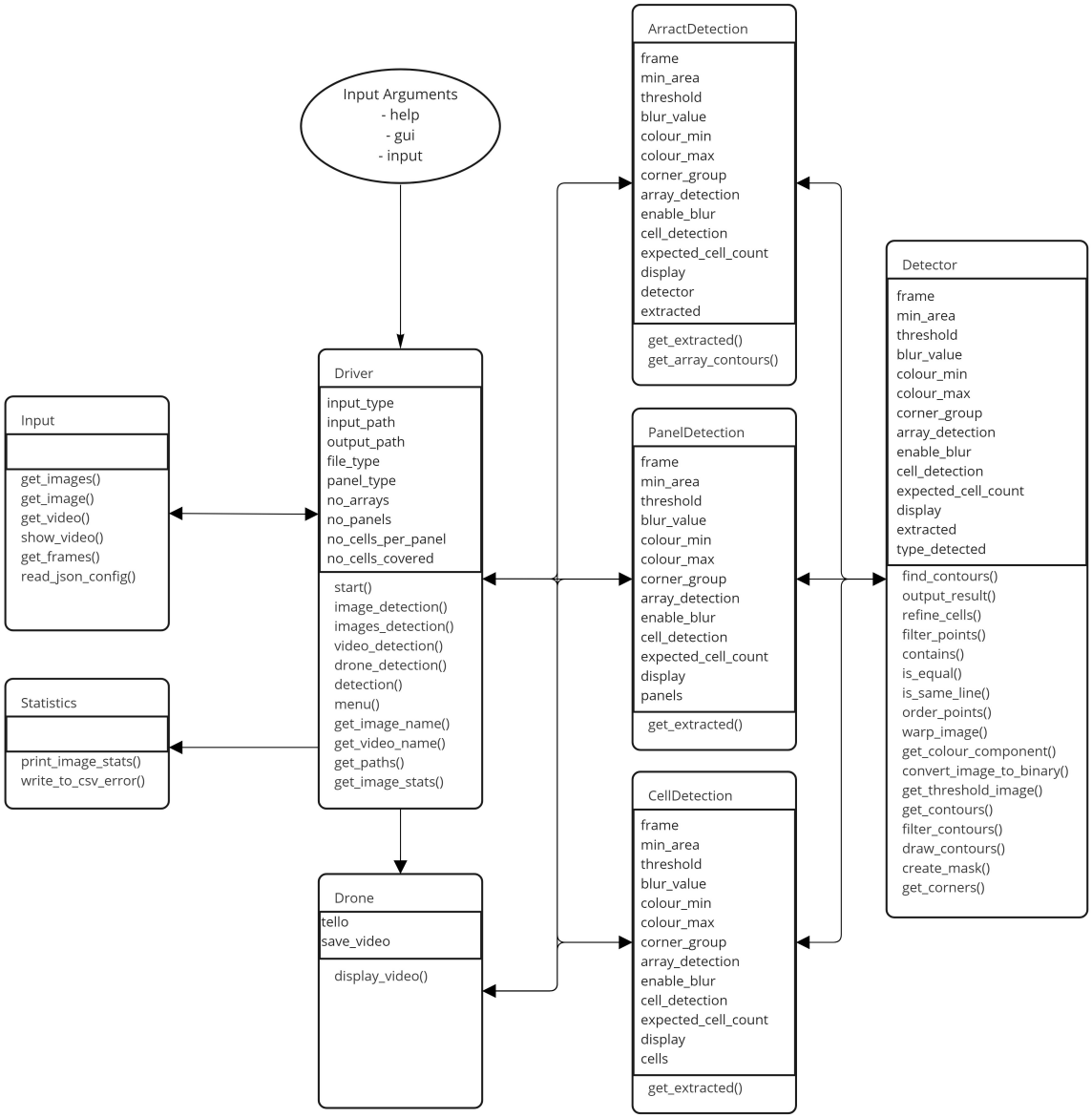

Fig. 3. TRANSECT: Full System Architecture

Fig. 4. DJI Tello Drone

IV. System Evaluation

To evaluate the implemented system, it was tested with on a range of real deployed solar panels. The aim was primarily to test the systems ability to detect solar panels and arrays, and to evaluate system performance.

A. Detection of Solar Panels

Different color ranges are used for detecting the different areas of the solar panel arrays. To achieve optimal detection rates of blue arrays the lower boundary saturation and lightness values were raised, to distinguish between arrays positioned close together. All of the HSV values of the lower boundary black threshold were raised, since black solar panels are not a perfect black color, they often contain hints of grey and blue. The color range adjustments made are displayed in Table II.

The blur kernel size was increased to 15, to ensure that all the panels with in the array are detected. The minimum contour area is not utilised in this stage of the detection, because the system sorts the contours by area and selects the largest to perform further detection on.

Each of the blue and black color thresholds were modified

Listing 1 input.json file example

```
{
    "_comment_input_type": "IMAGE=1
    , IMAGES=2, VIDEO=3, DRONE=4",
    "input_type":4,
    "input_path":"./input",
    "output_path":"./output",
    "_comment_file_type": "JPG=1,
    PNG=2, MP4=3",
    "file_type":3,
    "_comment_panel_type": "BLUE=1,
    BLACK=2",
    "panel_type":1,
    "no_arrays":1,
    "no_panels":12,
    "no_cells_per_panel":60,
    "no_cells_covered":0
}
```

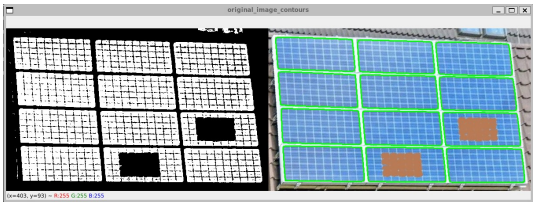

Fig. 5. System Detecting Panels with soiling.

for the detection of panels with in the given array, as seen in Table III, to improve the algorithms ability to establish the difference between the light colored borders of the panels, the base color of the panels and the shadows under them. The minimum contour area was lowered to detect panels that are further from the camera or in slightly lower resolution images.

The color ranges used to detect the cells of both blue and black panels was narrowed, to achieve higher rates of cell edge detection, they were narrowed to the values presented in Table IV. The blurring step was also disabled for this detection step because of the narrow borders between the cells being easily removed by the blurring process.

The system determines how much of a solar panel is compromised by soiling by comparing the expected number of cells to the detected number of cells. Figure 5 shows the system detecting each panel in an input array. The panels that are affected by soiling are passed to the cell detection component of the system which fails to detect the affected cells, displayed in Figure 6.

B. System Evaluation

The system architecture is efficient when analysing single images or smaller collections of images. However the efficiency can be improved when analysing videos, it currently attempts to detect solar panel arrays on every frame of the video, this leads to the system analysing many similar or even the same frames. The flexibility of the system could

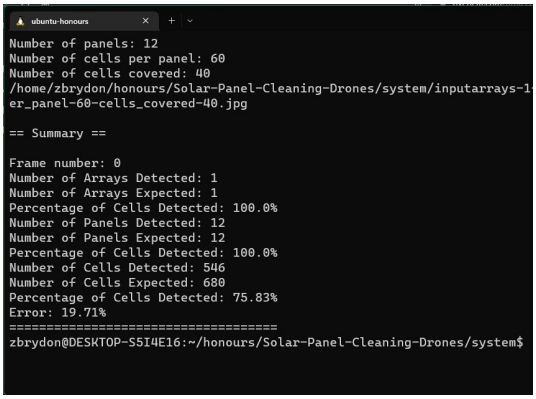

Fig. 6. The number of cells detected.

be improved by initially detecting multiple arrays instead of taking the largest contour each time and that step of the detection process. This would allow the system to detect multiple arrays while also improving detection accuracy for arrays that are segmented due to heavy soiling.

The detected results and expected results were saved and graphed, resulting in the graph presented in Figure 7. It displays a general trend that the system fairly accurately detected cells when the number of cells covered is below 180 (approx. three panels). As the number of cells covered by the simulated soiling increases the systems accuracy decreases.

There is a few notable outliers present, which are caused by the presence of the simulated soiling in a pattern which happens to split the solar array into multiple sections, like that in Figure 8. When detecting an array the system selects the largest area, which in this case would be the two panels in the bottom left corner of the image. The system then moves straight to detecting the panels within the array without checking if the original image contains multiple arrays.

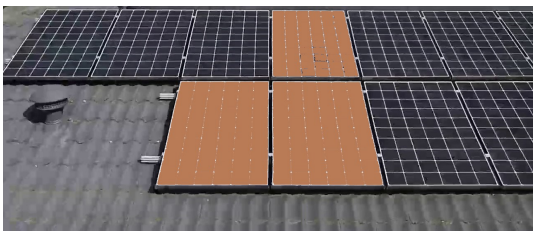

Fig. 8. Multiple Panel sections visible

C. Discussion of real-world suitability

The system was deployed on a physical solar panel installation in optimal lighting conditions, displayed in Figure 9.Video of the solar panels was captured by the drone's camera, each frame was then passed into the system.

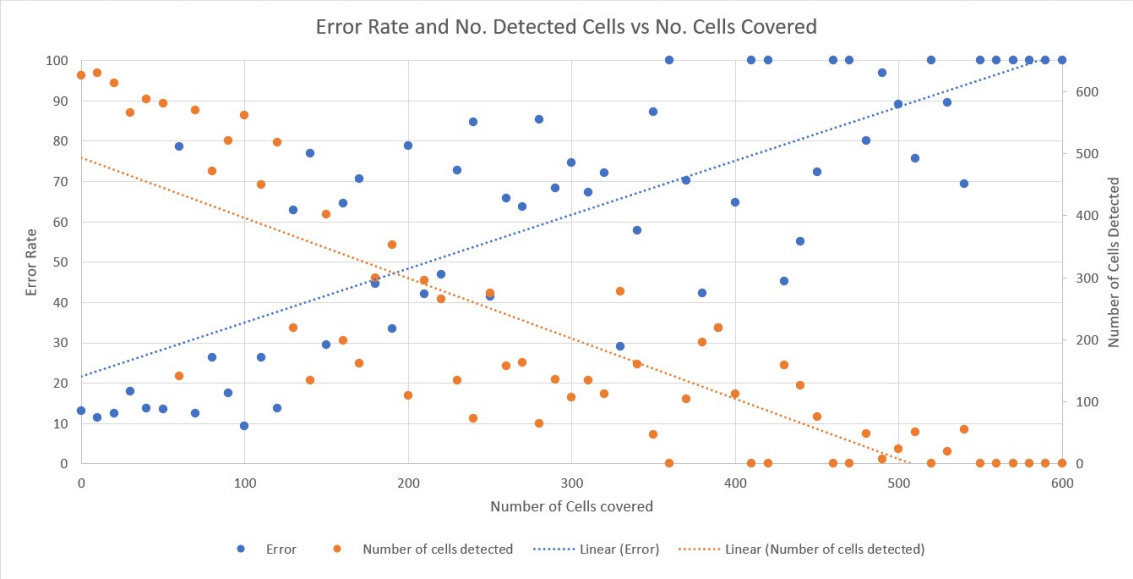

Fig. 7. Error Rate and No. Detected Cells vs No. of Cells Covered

Fig. 9. Deployment Conditions

The system performs well in certain frames, as illustrated in Figures 10 and 11, but fails to detect accurately in others due to the less than ideal panel installation environment. The black panels on a black tiled roof, with other black objects present such as solar pool heating, makes it difficult for the array detection algorithm to find the four corners of the array of panels. This is shown in Figure 12, where the algorithm mistakenly includes some of the solar pool heating in the detected array area.

Fig. 10. Accurate Detection Example

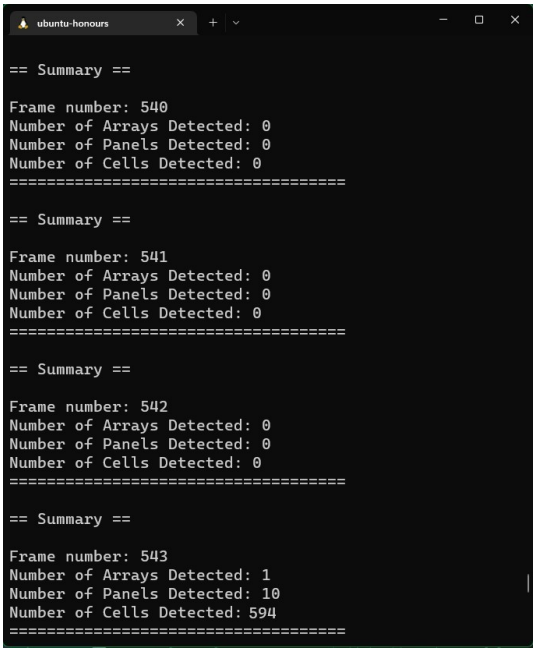

Fig. 11. Accurate Detection Results

There are several limitations introduced by the utilisation of a small commercial drone, as follows.

- The battery capacity (1100mAh) of the drone is too small for sustained flight and video capture/streaming for more than five to ten minutes, making it not be suitable for a commercial deployment of this system.
- The video is streamed via Wi-Fi from the drone, meaning the the drone cannot travel far from the controlling device and obstacles between it and the controlling device impact the quality of the signal.

- The drone camera is locked in a fixed horizontal position, limiting the systems ability to locate the panels which are affected by soiling since the position of the drone is not the same as the panel being detected.

The design limitation of the system in its current version is the lack of duplicate panel detection logic. Since the detection algorithm is running on each frame, the same panels are being detected multiple times, leading to unrealistically inflated panel detection counts.

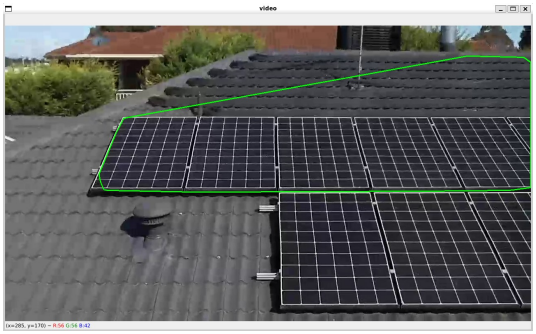

Fig. 12. Incorrect Detection

V. Conclusion

This paper has presented techniques and architecture for detecting solar panels and their physical status. It proposed an approach for a solar module detection system that determines the percentage of cells that are compromised by soiling. This system utilizes the three modules previously mentioned that detect arrays, panels and cells, outlined in the system diagram.

The major contribution of the research presented in this paper is the proposed combination of digital image processing methods and their respective parameters, employed to detect arrays, panels and cells of both blue and black photovoltaic panels. This was achieved by extracting the desired color threshold from an image, dynamically applying a Gaussian filter to the image to reduce the noise dependent on the target of the detection, a binary conversion, edge detection, corner detection and a final image re-projection.

In future work, the next step is to determine the optimal controllable environmental conditions for detecting solar panels and their faults in images and soiling condition, using the previously developed systems. The detection system has currently only been tested on one real world solar panel deployment, this provided a sound proof of concept for the systems viability. The next steps from here, is further testing on many different solar panel deployments, containing different solar panel types and installation surfaces. The addition of enabling the system to locate the solar panels that have been soiled, is a crucial next step in the development of a complete detection system that fills the gap in the current research.

References

[1] I. E. Agency, "World energy outlook 2021," in *World Energy Outlook 2021*, 2021.

[2] D. Feldman, K. Dummit, J. Zuboy, J. Heeter, K. Xu, and R. Margolis, "Spring 2022 solar industry update," in *Spring 2022 Solar Industry Update*, 2022.

[3] VDMA, "International technology roadmap for photovoltaic (itrpv) 2018 results," in *International Technology Roadmap for Photovoltaic (ITRPV) 2018 Results*, 2018.

[4] G. Shepherd, A. B. Utchang Kang Enric Terradellas, S. N. W. A. Sprigg, and A. A.-D. A. D. Boloorani, "Global assessment of sand and dust storms," *United Nations Enviromental Program*, p. 139, 2016.

[5] C. Schill, S. Brachmann, and M. Koehl, "Impact of soiling on iv-curves and efficiency of pv-modules," *Solar Energy*, vol. 112, pp. 259–262, 2015.

[6] M. G. Moheyer, M. A. Ramos, E. R. Sandoval, N. Pitalua-Diaz, R. Asomoza, G. Romero-Paredes, and Y. Matsumoto, "Notable changes in the performance of a photovoltaic system due to the dirt and cleaning cycles of pv-array," in *Notable changes in the performance of a photovoltaic system due to the dirt and cleaning cycles of PV-array*, pp. 656–659, Institute of Electrical and Electronics Engineers Inc., 6 2021.

[7] J. Canny, "A computational approach to edge detection," *IEEE Transactions on Pattern Analysis and Machine Intelligence*, vol. PAMI-8, no. 6, pp. 679–698, 1986.

[8] H. Razalli, R. Ramli, and M. H. Alkawaz, "Emergency vehicle recognition and classification method using hsv color segmentation," *Proceedings - 2020 16th IEEE International Colloquium on Signal Processing and its Applications, CSPA 2020*, pp. 284–289, 2 2020.

[9] G. Deng and L. Cahill, "An adaptive gaussian filter for noise reduction and edge detection," in *1993 IEEE Conference Record Nuclear Science Symposium and Medical Imaging Conference*, pp. 1615–1619 vol.3, 1993.

[10] S. Suzuki and K. be, "Topological structural analysis of digitized binary images by border following," *Computer Vision, Graphics, and Image Processing*, vol. 30, no. 1, pp. 32–46, 1985.

[11] T. Pivem, F. de Oliveira de Araujo, L. de Oliveira de Araujo, and G. S. de Oliveira, "Application of a computer vision method for soiling recognition in photovoltaic modules for autonomous cleaning ... related papers," *Signal and Image Processing: An International Journal (SIPIJ)*, vol. 10, 2019.

[12] W. Yap, R. Galet, and K. Yeo, "Quantitative analysis of dust and soiling on solar pv panels in the tropics utilizing image-processing methods," in *Proceedings of the Asia Pacific Solar Research Conference 2015* (R. Egan and R. Passey, eds.), pp. –, Australian PV Institute, 2015. Asia Pacific Solar Research Conference (2015), APSRC ; Conference date: 29-11-2016 Through 01-12-2016.

[13] H.-Y. Lee, "Generation of photo-mosaic images through block matching and color adjustment," *International Journal of Computer and Information Engineering*, vol. 8, no. 3, pp. 457 – 460, 2014.

[14] S. Mehta, A. P. Azad, S. A. Chemmengath, V. Raykar, and S. Kalyanaraman, "Deepsolareye: Power loss prediction and weakly supervised soiling localization via fully convolutional networks for solar panels," *Proceedings - 2018 IEEE Winter Conference on Applications of Computer Vision, WACV 2018*, vol. 2018-January, pp. 333–342, 5 2018.

[15] A. S. Shihavuddin, M. R. A. Rashid, M. H. Maruf, M. A. Hasan, M. A. ul Haq, R. H. Ashique, and A. A. Mansur, "Image based surface damage detection of renewable energy installations using a unified deep learning approach," *Energy Reports*, vol. 7, pp. 4566–4576, 11 2021.

[16] M. Tan, R. Pang, and Q. V. Le, "Efficientdet: Scalable and efficient object detection," in *Proceedings of the IEEE/CVF Conference on Computer Vision and Pattern Recognition (CVPR)*, June 2020.

[17] R. Cavieres, R. Barraza, D. Estay, J. Bilbao, and P. Valdivia-Lefort, "Automatic soiling and partial shading assessment on pv modules through rgb images analysis," *Applied Energy*, vol. 306, p. 117964, 1 2022.

[18] C. Henry, S. Poudel, S. W. Lee, and H. Jeong, "Automatic detection system of deteriorated pv modules using drone with thermal camera," *Applied Sciences 2020, Vol. 10, Page 3802*, vol. 10, p. 3802, 5 2020.

[19] C. G. Harris and M. J. Stephens, "A combined corner and edge detector," in *Alvey Vision Conference*, 1988.

[20] W. Förstner and E. Gülch, "A fast operator for detection and precise location of distinct points, corners and circular features," *Isprs Intercommission Workshop Interlaken*, pp. 281–305, 1987.